Supplementary Materials for

Repurposing of World-Approved Drugs for Potential Inhibition against Human Carbonic Anhydrase I: A Computational Study

Nannan Zheng [1], Wanyun Jiang [1], Puyu Zhang [1], Le Ma[1], Junzhao Chen[1] and Haiyang Zhang [1,*]

[1] Department of Biological Science and Engineering, School of Chemistry and Biological Engineering, University of Science and Technology Beijing, 100083 Beijing, China
* Correspondence: zhanghy@ustb.edu.cn

Table S1. Toxicity prediction of the existing ligand in complex with hCA I in the PDB database

Residue name	PDB ID	q	ΔE_{dock}	Toxicity				
				dili	carcino	immuno	mutagen	cyto
949	5GMM	0	-9.0	N(53)	N(62)	N(89)	N(70)	N(67)
TOR	3LXE	0	-8.5	N(66)	N(52)	N(84)	Y(52)	N(72)
GZE	6I0J	0	-8.5	Y(57)	N(61)	N(55)	N(62)	N(70)
V14	5E2M	0	-8.2	N(72)	N(72)	N(98)	N(72)	N(64)
BZE	6EVR	0	-8.1	N(78)	N(65)	N(99)	N(76)	N(63)
IWE	7ZL5	0	-8.0	N(59)	N(53)	N(95)	N(69)	N(62)
N19	6EX1	0	-8.0	N(80)	N(64)	N(99)	N(80)	N(61)
D3B	6FAF	0	-8.0	Y(54)	N(58)	N(99)	N(78)	N(78)
3UG	4WUQ	0	-8.0	N(66)	N(58)	N(99)	N(81)	N(69)
CJK	6F3B	0	-7.7	N(59)	N(64)	N(99)	N(79)	N(72)
O5N	6XZY	0	-7.7	N(65)	N(73)	N(90)	N(78)	N(68)
EON	6FAG	0	-7.6	Y(57)	N(57)	N(88)	N(73)	N(82)
O5H	6XZX	0	-7.5	N(70)	N(69)	N(99)	N(81)	N(64)
84Z	7Q0D	0	-7.4	N(65)	N(67)	N(99)	N(75)	N(70)
O4Z	6XZE	0	-7.3	N(65)	N(73)	N(93)	N(78)	N(68)
O5K	6XZS	0	-7.2	N(64)	N(72)	N(97)	N(82)	N(68)
3TV	4WR7	0	-7.1	N(75)	N(66)	N(98)	N(69)	N(78)
O55	6XZO	0	-7.0	N(65)	N(66)	Y(62)	N(74)	N(65)
7TI	7PLF	0	-6.9	N(74)	N(65)	N(95)	N(75)	N(76)
FLB	3W6I	0	-6.8	N(84)	N(53)	N(86)	N(76)	N(78)
O5T	6Y00	0	-6.7	N(65)	N(66)	Y(63)	N(74)	N(65)
M25	2NMX	0	-6.7	N(82)	N(73)	N(99)	N(79)	N(75)
M29	2NN7	0	-6.6	N(72)	N(64)	N(99)	N(69)	N(74)
M28	2NN1	0	-6.4	N(71)	N(67)	N(99)	N(73)	N(67)
AZM	3W6H	0	-6.3	N(56)	Y(51)	N(99)	N(85)	N(54)
MZM	1BZM	0	-6.3	N(81)	Y(50)	N(99)	N(70)	N(64)
AZM	1AZM	0	-5.9	N(56)	Y(51)	N(99)	N(85)	N(54)

3UF	4WUP	0	-5.7	N(82)	N(65)	N(99)	N(72)	N(75)
FO9	6G3V	0	-5.7	N(69)	Y(58)	N(99)	N(64)	N(54)
AAS	1CZM	0	-5.6	N(61)	N(62)	N(91)	N(80)	N(72)
GZH	6I0L	0	-5.5	N(64)	N(77)	N(91)	N(82)	N(77)
HIS	2FW4	1	-5.2	N(67)	N(80)	N(99)	N(66)	N(71)
PPF	2IT4	0	-4.3	N(94)	N(59)	N(99)	N(84)	N(70)
EDO	1JV0	0	-3.2	N(98)	N(86)	N(99)	N(94)	N(82)
BCT	1HCB	-1	-3.1	N(91)	N(63)	N(99)	N(88)	N(79)
EDO	1J9W	0	-1.7	N(98)	N(86)	N(99)	N(94)	N(82)

Table S2. Toxicity prediction of 79 compounds with ΔE_{dock} <= -9 kcal/mol and Zn^{2+}–ligand binding distances <= 3.5 Å from word-approved drugs

ZINC ID	Molecular structure	*q*	ΔE_{dock}	Toxicity				
				dili	carcino	immuno	mutagen	cyto
ZINC000164760756	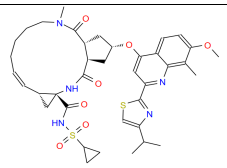	-1	-10.6	N(54)	N(59)	Y(92)	N(66)	N(52)
ZINC000003927200	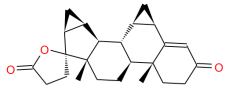	0	-10.4	N(79)	Y(66)	Y(89)	N(95)	N(83)
ZINC000060392779	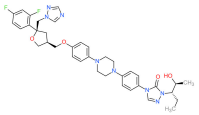	0	-10.2	Y(86)	N(62)	Y(99)	N(56)	N(75)
ZINC000012503149	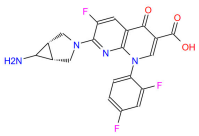	0	-10.2	Y(85)	Y(58)	Y(67)	Y(61)	N(89)
ZINC000100030989	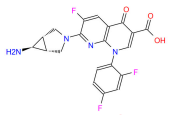	0	-10.2	Y(85)	Y(58)	Y(67)	Y(61)	N(89)
ZINC000147175374	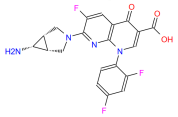	0	-10.2	Y(85)	Y(58)	Y(67)	Y(61)	N(89)
ZINC000095618351	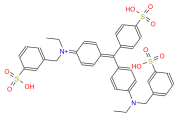	0	-10.1	N(70)	Y(53)	N(88)	Y(69)	N(58)
ZINC000003932831	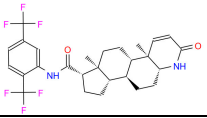	0	-10.1	N(92)	N(60)	Y(99)	N(64)	N(77)

ZINC000100067477	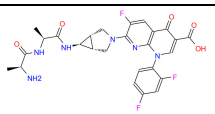	-1	-10	Y(85)	N(51)	N(57)	N(55)	N(70)
ZINC000100067477	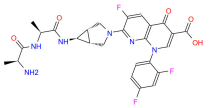	0	-10	Y(85)	N(51)	N(57)	N(55)	N(70)
ZINC000011679756	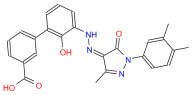	-3	-10	Y(67)	N(57)	N(72)	N(56)	N(84)
ZINC000011679756	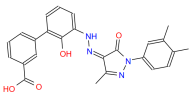	-2	-10	Y(67)	N(57)	N(72)	N(56)	N(84)
ZINC000014880001	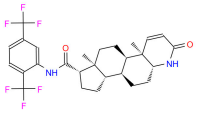	0	-10	N(92)	N(60)	Y(99)	N(64)	N(77)
ZINC000095618741	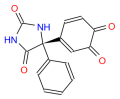	0	-9.9	Y(67)	Y(55)	N(98)	N(70)	N(66)
ZINC000011681563	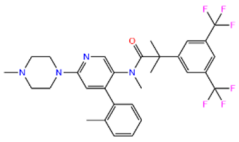	0	-9.9	N(66)	N(71)	N(78)	N(73)	N(64)
ZINC000011681563	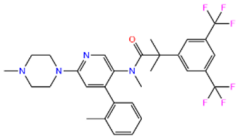	1	-9.9	N(66)	N(71)	N(78)	N(73)	N(64)
ZINC000936069565	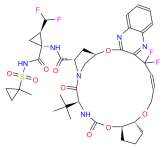	0	-9.9	Y(56)	N(58)	Y(96)	N(64)	N(50)
ZINC000004217252	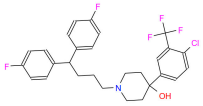	0	-9.9	N(94)	N(59)	Y(85)	N(83)	N(76)
ZINC000004217252	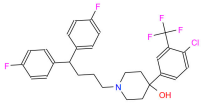	1	-9.9	N(94)	N(59)	Y(85)	N(83)	N(76)
ZINC000000601301	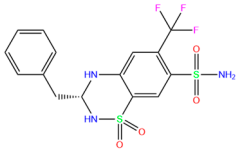	0	-9.8	N82)	N(71)	N(89)	N(84)	N73)
ZINC000205224698	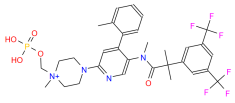	1	-9.8	N(66)	N(58)	N(53)	N(55)	N(61)
ZINC000004175630	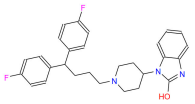	0	-9.8	N(78)	N(69)	Y(89)	N(86)	N(65)
ZINC000000538337	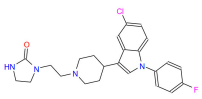	0	-9.8	N(75)	N(67)	Y(77)	N(56)	N(67)
ZINC000000538337	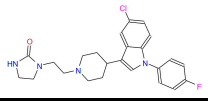	1	-9.8	N(75)	N(67)	Y(77)	N(56)	N(67)

ZINC000006716957	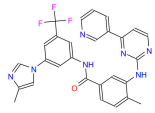	1	-9.7	Y(82)	Y(53)	Y(98)	N(59)	N(72)
ZINC000027990463	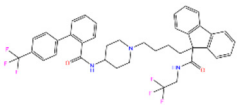	1	-9.7	N(78)	N(61)	N(70)	N(58)	N(77)
ZINC000000537755	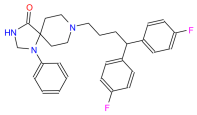	1	-9.7	N(74)	N(57)	Y(73)	N(69)	N(74)
ZINC000004175630	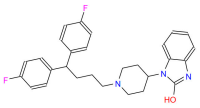	1	-9.7	N(78)	N(69)	Y(89)	N(86)	N(65)
ZINC000085599303	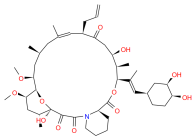	0	-9.7	N(83)	N(50)	Y(99)	N(73)	N(71)
ZINC000095618739	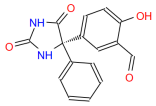	0	-9.6	Y(71)	Y(51)	N(96)	N(82)	N(74)
ZINC000685933136	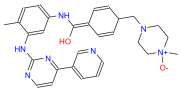	1	-9.6	N(55)	Y(52)	Y(80)	N(51)	N(63)
ZINC000021981256	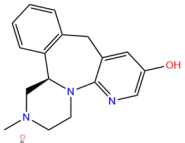	1	-9.6	N(83)	N(66)	N(96)	N(61)	N(59)
ZINC000003816514	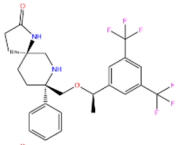	0	-9.6	N(83)	N(66)	N(93)	N(67)	N(75)
ZINC000003816514	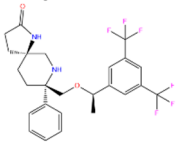	1	-9.6	N(83)	N(66)	N(93)	N(67)	N(75)
ZINC000261494552	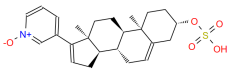	-1	-9.6	N(56)	N(68)	Y(82)	N(57)	N(65)
ZINC000006716957	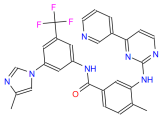	0	-9.5	Y(82)	Y(53)	Y(98)	N(59)	N(72)
ZINC000095618742	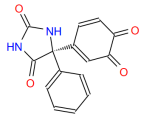	0	-9.5	Y(67)	Y(55)	N(98)	N(70)	N(66)
ZINC000011617039	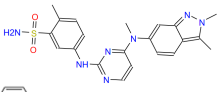	0	-9.5	N(65)	Y(66)	Y(85)	N(70)	Y(50)
ZINC000022034381	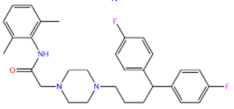	0	-9.5	N(79)	N(70)	N(97)	N(78)	N(67)
ZINC000095618852	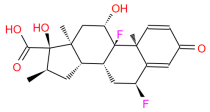	-1	-9.5	N(83)	Y(61)	Y(99)	N(76)	N(74)

ZINC000040165218	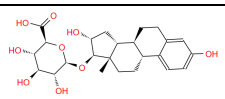	-1	-9.5	N(85)	N(66)	Y(99)	N(81)	N(64)
ZINC000261494710	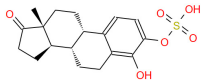	-1	-9.5	N(71)	N(77)	Y(82)	N(62)	N(78)
ZINC000257459143	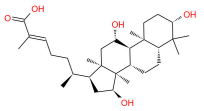	0	-9.5	N(58)	N(50)	Y(97)	N(71)	N(82)
ZINC000053073961	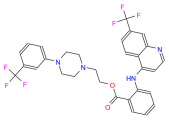	1	-9.4	N(78)	N(55)	Y(98)	N(65)	N(70)
ZINC000150338819	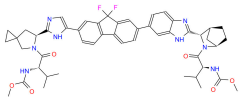	0	-9.4	N(63)	N(63)	Y(83)	N(67)	N(56)
ZINC000000020243	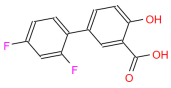	-1	-9.4	Y(75)	N(65)	N(97)	N(85)	N(60)
ZINC000100048501	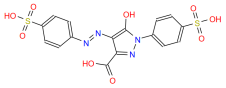	-4	-9.4	Y(51)	N(65)	N(99)	N(82)	N(66)
ZINC000003881958	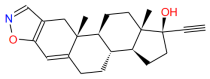	0	-9.4	Y(73)	N(60)	Y(78)	N(66)	N(76)
ZINC000031417974	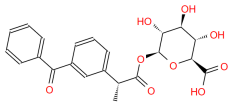	-1	-9.3	N(71)	N(68)	N(85)	N(85)	N(82)
ZINC000261494712	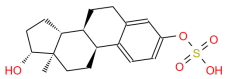	-1	-9.3	N(73)	N(78)	Y(99)	N(63)	N(75)
ZINC000031622970	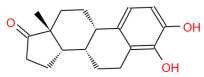	0	-9.3	N(70)	N(61)	Y(73)	N(89)	N(83)
ZINC000003873362	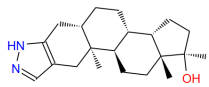	0	-9.3	N(53)	N(52)	Y(96)	N(67)	N(75)
ZINC000100051684	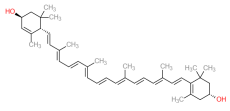	0	-9.3	N(79)	N(67)	Y(66)	N(81)	N(89)
ZINC000095862733	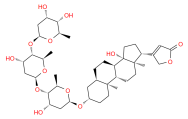	0	-9.3	N(96)	N(62)	Y(99)	N(93)	Y(59)
ZINC000100015190	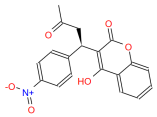	-1	-9.2	Y(51)	N(50)	N(95)	Y(85)	N(65)
ZINC000000601275	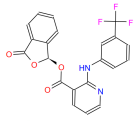	0	-9.2	Y(60)	Y(58)	N(52)	N(58)	N(70)
ZINC000002570882	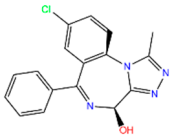	0	-9.2	N(52)	N(67)	N(97)	N(74)	N(70)

ZINC000004311748	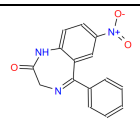	0	-9.2	N(50)	Y(61)	N(99)	N(65)	N(55)
ZINC000000607726	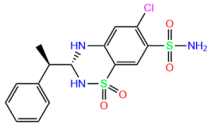	0	-9.2	N(89)	N(76)	N(88)	N(92)	N(81)
ZINC000022034381	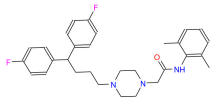	1	-9.2	N(79)	N(70)	N(97)	N(78)	N(67)
ZINC000001539579	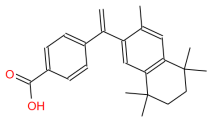	-1	-9.2	Y(80)	N(66)	N(99)	N(69)	N(79)
ZINC000095618879	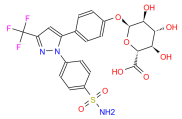	0	-9.2	Y(60)	Y(53)	N(70)	N(67)	N(79)
ZINC000118915338	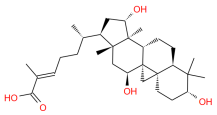	0	-9.2	N(58)	N(51)	Y(53)	N(60)	N(71)
ZINC000004026419	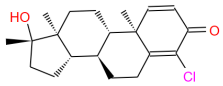	0	-9.2	Y(68)	Y(50)	Y(92)	N(92)	N(74)
ZINC000003873364	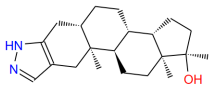	0	-9.2	N(53)	N(52)	Y(96)	N(67)	N(75)
ZINC000004215629	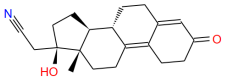	0	-9.2	Y(52)	N(72)	Y(61)	N(89)	N(81)
ZINC000000538152	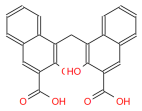	-2	-9.1	N(75)	N(71)	N(99)	N(62)	N(90)
ZINC000204073689	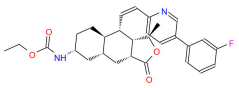	0	-9.1	N(62)	N(55)	Y(99)	N(58)	N(60)
ZINC000002017901	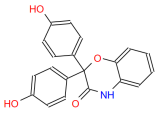	0	-9.1	Y(57)	Y(52)	N(99)	N(59)	N(69)
ZINC000000601254	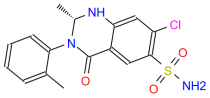	0	-9.1	N(65)	N(64)	N(73)	N(85)	Y(52)
ZINC000100053593	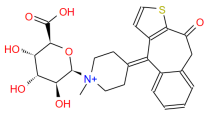	0	-9.1	N(71)	N(55)	N(82)	N(64)	N(51)
ZINC000043131420	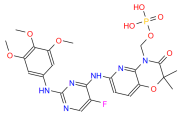	-2	-9.1	N(55)	N(65)	Y(99)	N(65)	N(61)
ZINC000085537142	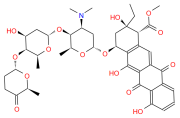	0	-9.1	N(71)	N(71)	Y(99)	Y(89)	N(57)

ZINC000085537142	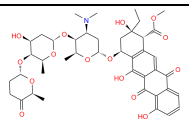	0	-9.1	N(71)	N(71)	Y(99)	Y(89)	N(57)
ZINC000033963989	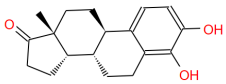	0	-9.1	N(70)	N(61)	Y(73)	N(89)	N(83)
ZINC000003875469	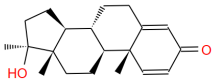	0	-9.1	Y(67)	N(56)	Y(97)	N(98)	N(89)
ZINC000261494708	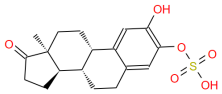	-1	-9.1	N(70)	N(76)	Y(98)	N(62)	N(78)
ZINC000100036907	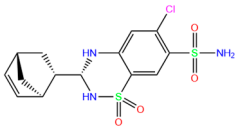	0	-9.1	N(91)	N(74)	N(91)	N(88)	N(73)
ZINC000242548690	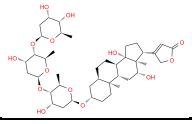	0	-9.1	N(98)	N(67)	Y(99)	N(59)	Y(59)

Table S3. Energy decomposition (kcal/mol) of identified key residues for binding with 84Z

Residue	ΔE_{vdW}	ΔE_{elec}	ΔE_{MM}	ΔG_{sol}	ΔE_{bind}
HIS-64	-0.1 ± -0.0	0.3 ± -0.1	0.3 ± -0.1	-0.4 ± -0.1	-0.1 ± -0.1
HIS-67	-0.1 ± -0.1	-0.1 ± -0.1	-0.2 ± -0.1	0.1 ± -0.1	-0.1 ± -0.1
GLN-92	-1.2 ± -0.3	0.6 ± -0.8	-0.6 ± -0.9	-1.1 ± -0.8	-1.7 ± -0.8
HIS-94	-1.3 ± -0.3	1.6 ± -0.8	0.3 ± -0.8	-2.1 ± -0.9	-1.8 ± -0.9
HIS-96	-0.2 ± -0.0	1.5 ± -0.2	1.3 ± -0.2	-2.5 ± -0.4	-1.3 ± -0.5
GLU-106	-0.3 ± -0.1	1.7 ± -1.1	1.3 ± -1.1	0.8 ± -1.9	2.2 ± -1.9
HIS-107	-0.1 ± -0.0	-1.9 ± -0.4	-2.0 ± -0.4	1.3 ± -0.5	-0.7 ± -0.5
GLU-117	-0.0 ± -0.0	1.9 ± -0.3	1.9 ± -0.3	-1.9 ± -0.4	0.0 ± -0.4
HIS-119	-0.9 ± -0.3	3.1 ± -0.6	2.1 ± -0.8	-3.6 ± -1.1	-1.5 ± -1.3
ALA-121	-0.9 ± -0.2	-0.6 ± -0.2	-1.5 ± -0.3	0.9 ± -0.4	-0.5 ± -0.4
HIS-122	-0.2 ± -0.1	-1.9 ± -0.3	-2.1 ± -0.3	3.1 ± -0.8	1.0 ± -0.7
LEU-131	-0.3 ± -0.2	-0.1 ± -0.1	-0.4 ± -0.3	0.1 ± -0.1	-0.3 ± -0.2
ALA-132	-0.0 ± -0.0	-0.1 ± -0.0	-0.1 ± -0.0	0.1 ± -0.0	-0.0 ± -0.0
ALA-135	-0.3 ± -0.2	-0.2 ± -0.2	-0.6 ± -0.3	0.4 ± -0.4	-0.1 ± -0.2
LEU-141	-1.3 ± -0.4	-0.5 ± -0.3	-1.8 ± -0.6	0.8 ± -0.4	-1.0 ± -0.4
VAL-143	-1.3 ± -0.5	-0.1 ± -0.1	-1.4 ± -0.4	0.5 ± -0.1	-0.9 ± -0.5
LEU-198	-2.2 ± -0.4	-0.0 ± -0.2	-2.3 ± -0.5	0.5 ± -0.2	-1.8 ± -0.5
THR-199	-0.5 ± -0.5	-3.5 ± -0.9	-4.0 ± -0.7	1.3 ± -0.4	-2.7 ± -0.6
HIS-200	-1.3 ± -0.7	-3.5 ± -1.5	-4.8 ± -1.2	2.4 ± -0.6	-2.3 ± -1.3
PRO-201	-0.1 ± -0.0	-0.4 ± -0.1	-0.5 ± -0.1	0.3 ± -0.1	-0.1 ± -0.1
PRO-202	-0.2 ± -0.1	0.2 ± -0.1	0.0 ± -0.1	-0.1 ± -0.0	-0.1 ± -0.1
TRP-209	-0.8 ± -0.3	-1.8 ± -1.1	-2.7 ± -1.1	1.1 ± -0.5	-1.5 ± -0.8
ZN-261	0.9 ± -0.6	-20.3 ± -2.8	-19.4 ± -2.4	38.7 ± -5.2	19.3 ± -5.7

Table S4. Energy decomposition (kcal/mol) of identified key residues for binding with cyclothiazide

Residue	ΔE_{vdW}	ΔE_{elec}	ΔE_{MM}	ΔG_{sol}	ΔE_{bind}
HIS-64	-0.8 ± -0.4	-0.6 ± -1.6	-1.4 ± -1.6	0.9 ± -1.0	-0.5 ± -0.8
HIS-67	-1.5 ± -0.5	-0.6 ± -0.9	-2.2 ± -1.2	1.0 ± -0.7	-1.2 ± -1.1
GLN-92	-1.5 ± -0.5	-0.3 ± -1.0	-1.8 ± -1.0	0.0 ± -0.7	-1.8 ± -0.8
HIS-94	-2.0 ± -0.4	1.5 ± -0.8	-0.5 ± -1.0	-2.5 ± -1.4	-3.0 ± -1.7
HIS-96	-0.3 ± -0.0	1.3 ± -0.3	1.1 ± -0.3	-3.4 ± -1.3	-2.3 ± -1.3
GLU-106	-0.1 ± -0.0	3.0 ± -0.5	2.9 ± -0.5	-4.2 ± -1.1	-1.3 ± -1.1
HIS-107	-0.0 ± -0.0	-2.2 ± -0.2	-2.2 ± -0.2	2.5 ± -0.5	0.3 ± -0.5
GLU-117	-0.0 ± -0.0	2.2 ± -0.2	2.2 ± -0.2	-2.9 ± -0.5	-0.7 ± -0.5
HIS-119	-0.7 ± -0.1	3.2 ± -0.6	2.5 ± -0.6	-5.5 ± -1.1	-3.0 ± -1.1
ALA-121	-0.4 ± -0.1	-0.1 ± -0.1	-0.5 ± -0.1	0.4 ± -0.1	-0.1 ± -0.1
HIS-122	-0.1 ± -0.0	-0.1 ± -0.3	-0.2 ± -0.3	0.6 ± -0.3	0.4 ± -0.2
LEU-131	-0.1 ± -0.0	0.1 ± -0.1	-0.0 ± -0.1	-0.1 ± -0.1	-0.1 ± -0.0
ALA-132	-0.0 ± -0.0	-0.0 ± -0.0	-0.0 ± -0.0	0.0 ± -0.0	-0.0 ± -0.0
ALA-135	-0.1 ± -0.0	0.2 ± -0.1	0.1 ± -0.1	-0.2 ± -0.1	-0.1 ± -0.1
LEU-141	-0.4 ± -0.1	0.1 ± -0.1	-0.4 ± -0.1	0.2 ± -0.1	-0.2 ± -0.1
VAL-143	-0.7 ± -0.2	-0.2 ± -0.1	-0.9 ± -0.2	0.3 ± -0.1	-0.6 ± -0.2
LEU-198	-1.8 ± -0.3	-0.4 ± -0.3	-2.2 ± -0.5	0.3 ± -0.2	-1.9 ± -0.5
THR-199	-0.7 ± -0.3	-2.0 ± -0.9	-2.7 ± -0.7	0.7 ± -0.5	-2.0 ± -0.7
HIS-200	-2.1 ± -0.6	-4.2 ± -0.7	-6.4 ± -0.7	4.2 ± -0.5	-2.2 ± -0.8
PRO-201	-0.4 ± -0.1	-0.5 ± -0.2	-0.9 ± -0.2	0.9 ± -0.3	0.0 ± -0.2
PRO-202	-0.4 ± -0.1	0.2 ± -0.1	-0.2 ± -0.1	-0.1 ± -0.1	-0.3 ± -0.1
TRP-209	-0.8 ± -0.2	0.1 ± -0.3	-0.8 ± -0.3	0.5 ± -0.1	-0.3 ± -0.3
ZN-261	0.4 ± -0.5	-20.4 ± -3.6	-19.9 ± -3.2	46.9 ± -10.7	26.9 ± -10.1

Table S5. Energy decomposition (kcal/mol) of identified key residues for binding with 3UG

Residue	ΔE_{vdW}	ΔE_{elec}	ΔE_{MM}	ΔG_{sol}	ΔE_{bind}
HIS-64	-0.1 ± -0.0	0.6 ± -0.1	0.5 ± -0.1	-0.7 ± -0.1	-0.2 ± -0.1
HIS-67	-0.1 ± -0.0	-0.1 ± -0.1	-0.2 ± -0.1	0.2 ± -0.1	-0.0 ± -0.1
GLN-92	-0.9 ± -0.3	1.5 ± -0.5	0.5 ± -0.5	-1.5 ± -0.6	-1.0 ± -0.4
HIS-94	-0.2 ± -0.5	5.4 ± -1.2	5.2 ± -1.3	-7.3 ± -1.1	-2.1 ± -1.3
HIS-96	-0.5 ± -0.1	4.5 ± -0.6	3.9 ± -0.6	-7.1 ± -0.7	-3.1 ± -0.6
GLU-106	-0.1 ± -0.0	5.0 ± -0.6	4.9 ± -0.5	-6.4 ± -0.8	-1.6 ± -0.8
HIS-107	-0.0 ± -0.0	-2.9 ± -0.2	-2.9 ± -0.2	4.3 ± -0.4	1.3 ± -0.4
GLU-117	-0.0 ± -0.0	3.1 ± -0.2	3.0 ± -0.2	-4.7 ± -0.4	-1.6 ± -0.4
HIS-119	-0.8 ± -0.1	5.3 ± -0.7	4.5 ± -0.8	-8.4 ± -0.7	-3.9 ± -0.7
ALA-121	-0.4 ± -0.1	-0.1 ± -0.0	-0.5 ± -0.1	0.7 ± -0.3	0.2 ± -0.2
HIS-122	-0.1 ± -0.0	-0.4 ± -0.2	-0.4 ± -0.2	1.5 ± -0.6	1.1 ± -0.5
LEU-131	-0.6 ± -0.3	-0.0 ± -0.1	-0.7 ± -0.2	-0.0 ± -0.2	-0.7 ± -0.3
ALA-132	-0.1 ± -0.0	-0.1 ± -0.0	-0.1 ± -0.0	0.0 ± -0.0	-0.1 ± -0.0
ALA-135	-0.5 ± -0.2	0.1 ± -0.1	-0.4 ± -0.2	-0.3 ± -0.2	-0.7 ± -0.3
LEU-141	-0.8 ± -0.2	0.1 ± -0.1	-0.7 ± -0.2	0.6 ± -0.2	-0.2 ± -0.3
VAL-143	-0.6 ± -0.1	-0.3 ± -0.1	-0.8 ± -0.2	0.5 ± -0.1	-0.4 ± -0.2
LEU-198	-2.0 ± -0.5	-0.8 ± -0.2	-2.9 ± -0.5	1.4 ± -0.2	-1.5 ± -0.5
THR-199	-0.8 ± -0.1	-0.6 ± -0.4	-1.4 ± -0.4	1.5 ± -0.3	0.1 ± -0.4
HIS-200	-0.8 ± -0.7	-3.4 ± -0.9	-4.2 ± -0.7	2.2 ± -0.6	-2.1 ± -0.6
PRO-201	-0.3 ± -0.1	-0.1 ± -0.1	-0.4 ± -0.1	0.8 ± -0.3	0.3 ± -0.3
PRO-202	-0.7 ± -0.3	0.1 ± -0.1	-0.6 ± -0.3	0.2 ± -0.1	-0.4 ± -0.3
TRP-209	-0.6 ± -0.2	-0.5 ± -0.1	-1.1 ± -0.2	0.6 ± -0.1	-0.4 ± -0.2
ZN-261	1.8 ± -0.8	-45.8 ± -4.3	-44.0 ± -3.8	77.0 ± -4.7	33.0 ± -5.0

Table S6. Energy decomposition (kcal/mol) of identified key residues for binding with ketoprofen glucuronide

Residue	ΔE_{vdW}	ΔE_{elec}	ΔE_{MM}	ΔG_{sol}	ΔE_{bind}
HIS-64	-0.2 ± -0.1	-1.6 ± -0.3	-1.8 ± -0.3	1.4 ± -0.3	-0.4 ± -0.1
HIS-67	-0.2 ± -0.0	0.1 ± -0.5	-0.1 ± -0.5	-0.0 ± -0.4	-0.1 ± -0.2
GLN-92	-1.4 ± -0.2	1.0 ± -0.7	-0.4 ± -0.6	-0.3 ± -0.7	-0.8 ± -0.4
HIS-94	-0.5 ± -0.4	11.0 ± -1.0	10.5 ± -1.2	-9.5 ± -1.0	1.0 ± -1.1
HIS-96	-0.3 ± -0.0	8.4 ± -0.4	8.2 ± -0.4	-9.6 ± -0.9	-1.4 ± -0.8
GLU-106	-0.1 ± -0.0	24.6 ± -0.9	24.6 ± -0.9	-21.9 ± -1.0	2.6 ± -1.0
HIS-107	-0.0 ± -0.0	-18.9 ± -0.6	-18.9 ± -0.6	17.1 ± -0.7	-1.7 ± -0.5
GLU-117	-0.0 ± -0.0	19.5 ± -0.5	19.5 ± -0.5	-18.0 ± -0.7	1.5 ± -0.5
HIS-119	-0.7 ± -0.1	11.9 ± -1.2	11.2 ± -1.3	-11.2 ± -1.0	-0.0 ± -1.1
ALA-121	-1.2 ± -0.2	-1.6 ± -0.2	-2.8 ± -0.4	1.6 ± -0.4	-1.2 ± -0.4
HIS-122	-0.5 ± -0.1	-14.7 ± -0.5	-15.2 ± -0.5	16.3 ± -0.7	1.1 ± -0.6
LEU-131	-2.0 ± -0.3	0.5 ± -0.1	-1.4 ± -0.3	-0.2 ± -0.3	-1.6 ± -0.4
ALA-132	-0.7 ± -0.2	0.4 ± -0.1	-0.3 ± -0.3	-0.2 ± -0.1	-0.6 ± -0.3
ALA-135	-1.1 ± -0.2	0.8 ± -0.2	-0.3 ± -0.2	-0.5 ± -0.1	-0.8 ± -0.2
LEU-141	-1.1 ± -0.2	-1.2 ± -0.2	-2.4 ± -0.3	0.9 ± -0.2	-1.4 ± -0.3
VAL-143	-0.6 ± -0.1	-1.5 ± -0.3	-2.1 ± -0.3	1.3 ± -0.2	-0.8 ± -0.2
LEU-198	-1.8 ± -0.3	-3.2 ± -0.3	-5.0 ± -0.5	2.8 ± -0.2	-2.2 ± -0.5
THR-199	-0.3 ± -0.1	-1.0 ± -0.5	-1.4 ± -0.5	2.1 ± -0.4	0.7 ± -0.4
HIS-200	-1.2 ± -0.5	2.4 ± -1.1	1.1 ± -1.0	-0.3 ± -0.5	0.8 ± -0.8
PRO-201	-0.3 ± -0.1	1.1 ± -0.4	0.8 ± -0.4	-0.4 ± -0.4	0.4 ± -0.3
PRO-202	-0.8 ± -0.2	-0.9 ± -0.2	-1.7 ± -0.4	0.7 ± -0.2	-1.0 ± -0.3
TRP-209	-0.6 ± -0.1	-0.9 ± -0.5	-1.4 ± -0.5	1.1 ± -0.3	-0.3 ± -0.3
ZN-261	2.8 ± -1.0	-124.1 ± -3.8	-121.3 ± -3.0	131.0 ± -8.0	9.8 ± -7.8

Table S7. Energy decomposition (kcal/mol) of identified key residues for binding with bhft

Residue	ΔE_{vdW}	ΔE_{elec}	ΔE_{MM}	ΔG_{sol}	ΔE_{bind}
HIS-64	-0.1 ± -0.1	0.3 ± -0.2	0.1 ± -0.2	-0.3 ± -0.2	-0.2 ± -0.2
HIS-67	-0.3 ± -0.1	0.3 ± -0.2	-0.0 ± -0.3	-0.2 ± -0.5	-0.3 ± -0.3
GLN-92	-1.2 ± -0.4	-0.2 ± -0.7	-1.4 ± -0.9	1.2 ± -0.8	-0.2 ± -0.7
HIS-94	-0.6 ± -0.5	8.0 ± -1.2	7.4 ± -1.3	-9.7 ± -1.0	-2.3 ± -1.1
HIS-96	-0.5 ± -0.1	4.4 ± -0.5	3.9 ± -0.5	-7.1 ± -0.7	-3.2 ± -0.6
GLU-106	-0.1 ± -0.0	5.4 ± -0.6	5.3 ± -0.6	-6.1 ± -1.6	-0.8 ± -1.7
HIS-107	-0.0 ± -0.0	-3.2 ± -0.2	-3.2 ± -0.2	4.1 ± -0.6	0.9 ± -0.6
GLU-117	-0.0 ± -0.0	3.5 ± -0.2	3.5 ± -0.2	-4.8 ± -0.6	-1.4 ± -0.6
HIS-119	-1.0 ± -0.1	5.9 ± -0.7	4.9 ± -0.8	-8.3 ± -0.8	-3.3 ± -1.0
ALA-121	-0.3 ± -0.2	-0.0 ± -0.1	-0.3 ± -0.2	0.3 ± -0.1	-0.0 ± -0.2
HIS-122	-0.1 ± -0.0	0.1 ± -0.2	0.1 ± -0.2	0.6 ± -0.3	0.7 ± -0.3
LEU-131	-1.3 ± -0.5	-0.2 ± -0.4	-1.5 ± -0.7	0.8 ± -0.7	-0.7 ± -0.5
ALA-132	-0.8 ± -0.4	-0.0 ± -0.2	-0.8 ± -0.4	0.1 ± -0.2	-0.7 ± -0.4
ALA-135	-0.6 ± -0.2	0.5 ± -0.1	-0.1 ± -0.2	-0.4 ± -0.2	-0.6 ± -0.2
LEU-141	-0.7 ± -0.2	0.1 ± -0.1	-0.6 ± -0.2	0.3 ± -0.1	-0.2 ± -0.2
VAL-143	-0.6 ± -0.2	-0.3 ± -0.1	-0.9 ± -0.2	0.6 ± -0.1	-0.3 ± -0.3
LEU-198	-2.5 ± -0.3	-0.8 ± -0.2	-3.2 ± -0.4	1.4 ± -0.3	-1.8 ± -0.5
THR-199	-0.8 ± -0.1	-0.0 ± -0.4	-0.8 ± -0.4	1.1 ± -0.3	0.3 ± -0.5
HIS-200	-1.2 ± -0.7	-5.2 ± -1.0	-6.5 ± -0.8	4.2 ± -0.7	-2.2 ± -0.8
PRO-201	-0.4 ± -0.1	0.5 ± -0.3	0.1 ± -0.3	0.6 ± -0.4	0.7 ± -0.5
PRO-202	-0.7 ± -0.2	0.0 ± -0.2	-0.6 ± -0.2	0.1 ± -0.1	-0.5 ± -0.2
TRP-209	-0.7 ± -0.2	-0.4 ± -0.1	-1.1 ± -0.2	0.7 ± -0.2	-0.4 ± -0.2
ZN-261	2.2 ± -1.1	-51.3 ± -4.0	-49.1 ± -3.3	83.9 ± -5.0	34.8 ± -5.2

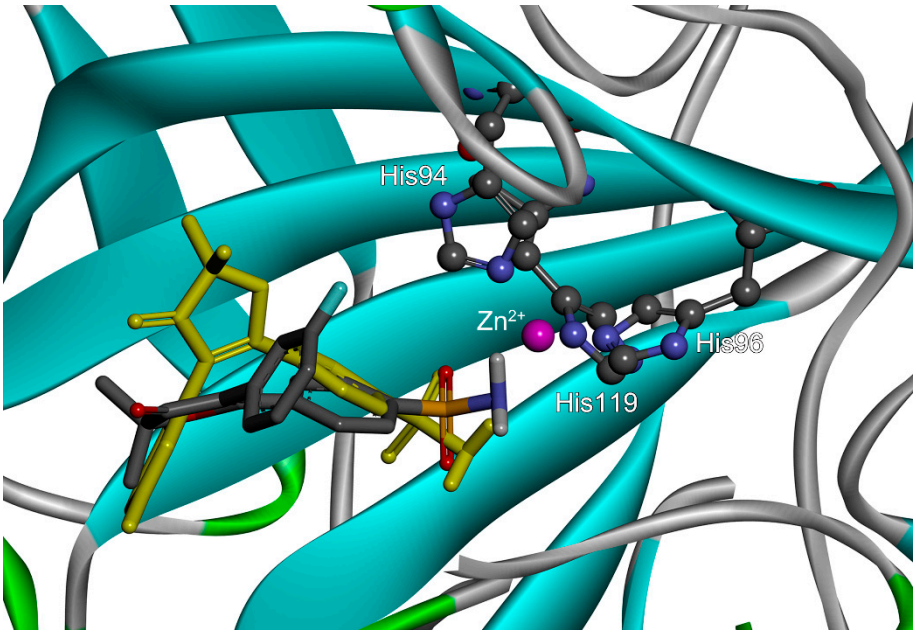

Figure S1. Comparison of crystal structure with docking pose for the binding of polmacoxib to hCA I. Crystal structure was taken from PDB database (PDB code: 5GMM). The crystal ligand was colored by element, and the docking pose was in yellow.

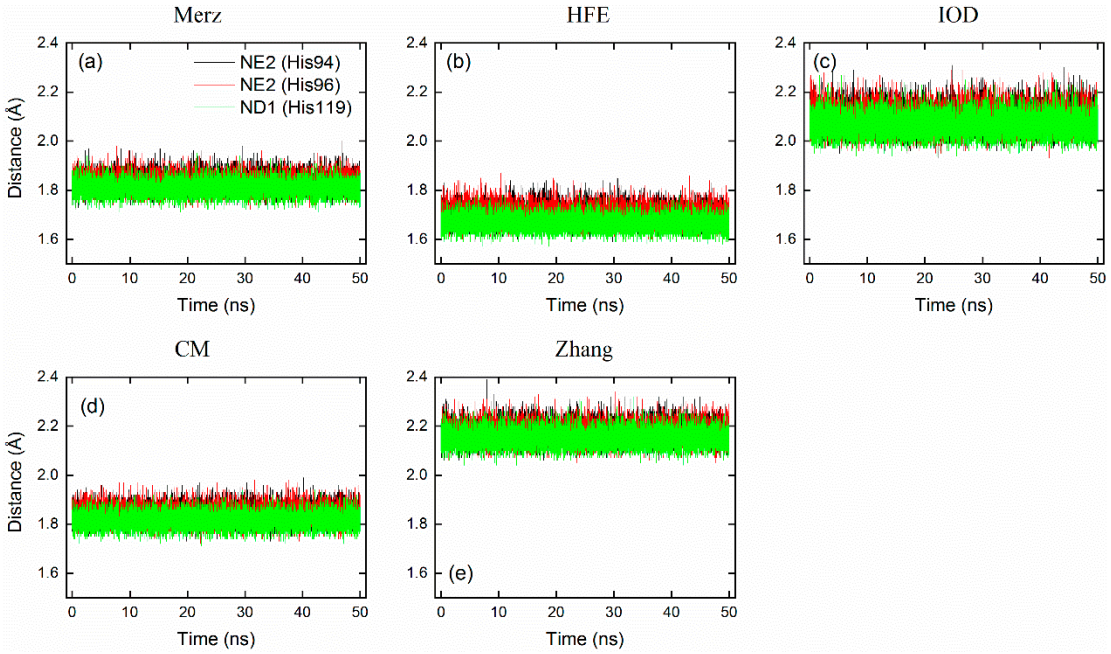

Figure S2. Zn^{2+}–ligand binding distance as a function of simulation time for ligand-free hCA I using modified Amber ff14SB protein force fields with different ion models (a-e). Refer to Table 3 in the main text for the details of force field parameters. Distances with the NE2 atom (black) of His94, the NE2 atom (red) of His96, and the ND1 atom (green) of His119 were monitored.

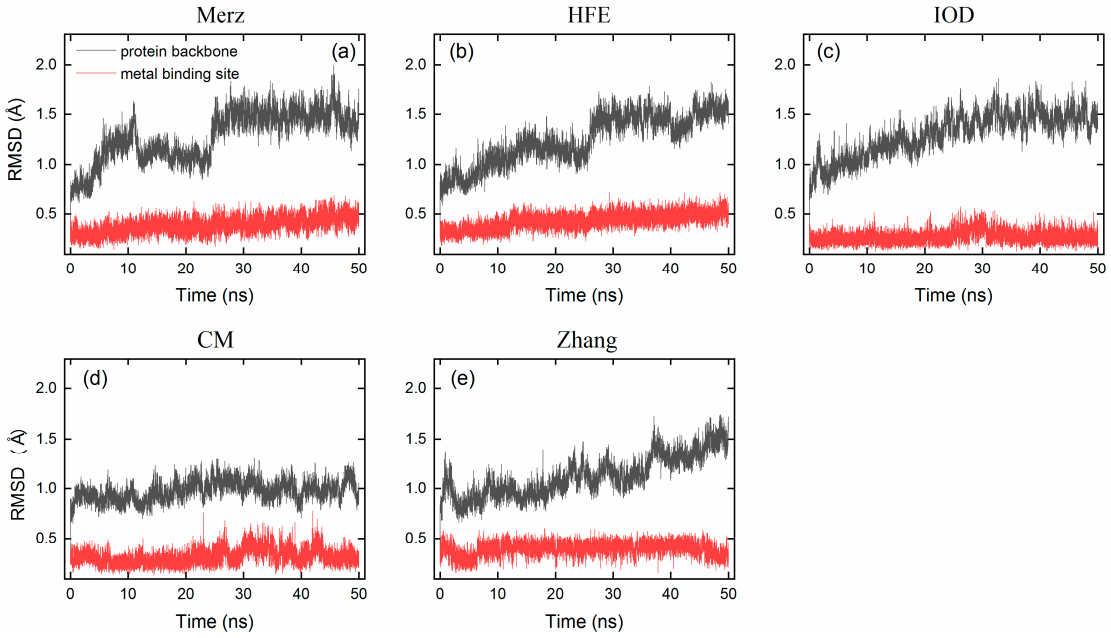

Figure S3. RMSD of hCA I protein backbone (black) and metal binding site (red) from crystal structure as a function of simulation time for ligand-free hCA I using modified Amber ff14SB protein force fields with different ion models (a-e). Refer to Table 3 for the details of force field parameters.